RSC Advances

PAPER

View Article Online
View Journal | View Issue

Cite this: *RSC Adv.*, 2019, **9**, 39824

Synthesis of a novel hexaazatriphenylene derivative for the selective detection of copper ions in aqueous solution†

Tahseen S. Saeed, ‡*[a] Dinesh Maddipatla, ‡*[b] Binu B. Narakathu,[b] Sarah S. Albalawi,[a] Sherine O. Obare[c] and Massood Z. Atashbar[b]

A hexaazatriphenylene (HAT) derivative, naphtho[2,3-h]naphtho[2′,3′:7,8]quinoxalino[2,3-*a*]naphtho[2′,3′:7,8]quinoxalino[2,3-*c*]phenazine-5,10,15,20,25,30-hexaone (NQH) was synthesized, characterized, and found to have novel properties in being selective toward the detection of copper (Cu^{2+}) ions. The capability of NQH to be employed as a colorimetric, chemo-fluorescence and electrochemical sensor for the detection of Cu^{2+} was demonstrated by performing UV-Vis absorbance, fluorescence intensity, and cyclic voltammetry (CV) measurements. The interaction between NQH and Cu^{2+} was initially observed with an obvious color change from yellow to brown upon the addition of Cu^{2+} ions to NQH. The interaction was also confirmed by UV-Vis absorbance, fluorescence intensity, and mass spectroscopy (MS/MS) measurements. UV absorbance, fluorescence and CV of NQH toward Cu^{2+} showed good linearity with a detection limit of 3.32 μM, 2.20 μM and 0.78 μM, respectively, which are lower than the toxicity levels of copper in drinking water (20–30 μM) set by the U.S. Environmental Protection Agency (EPA) and World Health Organization (WHO). A 1 : 2 stoichiometry complexation between NQH and Cu^{2+} was confirmed by Job's plot and MS/MS. In addition, the selectivity and sensitivity of the NQH compound towards Cu^{2+} ions were further confirmed by performing CV on a screen printed flexible and planar electrochemical sensor.

Received 27th October 2019
Accepted 7th November 2019

DOI: 10.1039/c9ra08825c

rsc.li/rsc-advances

1. Introduction

Heavy metals such as lead (Pb), cadmium (Cd), mercury (Hg), Arsenic (As) and copper (Cu) present in the environment impact biological species (humans, plants and animals) living in it.[1–3] Exposure to the heavy metals causes adverse health effects on the living organisms.[4,5] Among the various heavy metals, copper is a non-biodegradable metal and its ion (Cu^{2+}) an essential micronutrient that supports the fundamental physiological processes of living organisms.[6–8] However, the excessive consumption of Cu^{2+} may result in its accumulation in soft tissues causing many health and physiological diseases including ischemic heart disease, anemia, kidney and liver damage, gastrointestinal disturbance, severe intravascular hemolysis, hepatotoxicity and acute renal failure.[9–11] In addition, high exposure to Cu^{2+} can cause slow memory loss in elderly people with Wilson's disease.[11,12] Therefore, the accurate detection of Cu^{2+} ions in environmental and biological samples is very important.

Many techniques have been developed for the detection of Cu^{2+} ions including inductively coupled plasma atomic emission spectrometry (ICP-AES), atomic absorption spectrometry (AAS), inductively coupled plasma mass spectrometry (ICP-MS), chromatography, gravimetric detection and photometry.[13–19] However, most of these techniques are complex, bulky, time-consuming, non-portable and require relatively expensive apparatus as well as trained professionals to operate. To overcome these limitations, optical and electrochemical techniques such as UV-Vis, fluorescence, electrochemical impedance spectroscopy (EIS) and cyclic voltammetry (CV) can be used for the detection of Cu^{2+} ions cost effectively.[20,21] However, chemical compounds that exhibit both optical and electrochemical properties which are selective and sensitive only towards Cu^{2+} ions have not been explored well enough. So, there is a need to synthesize novel materials that possess both optical and electrochemical properties towards only Cu^{2+} ions, over other heavy metal ions.

Over the last decade, polycyclic aromatic hydrocarbons (PAH) have been receiving more attention in nanoscience and materials related fields for various applications due to their

[a]*Department of Chemistry, Western Michigan University, Kalamazoo, Michigan-49008, USA. E-mail: tahseensulaima.saeed@wmich.edu*

[b]*Department of Electrical and Computer Engineering, Western Michigan University, Kalamazoo, Michigan-49008, USA. E-mail: dinesh.maddipatla@wmich.edu*

[c]*Department of Nanoscience, Joint School of Nanoscience and Nanoengineering, University of North Carolina at Greensboro, Greensboro, NC 27401, USA*

† Electronic supplementary information (ESI) available. See DOI: 10.1039/c9ra08825c

‡ Dinesh Maddipatla and Tahseen S. Saeed contributed equally to this work, thus both should be considered as the first authors.

high charge-carrier mobility and tailorability.[22,23] However, it has been reported that some of the linear PAHs are not stable because of its narrow band gaps and low ionization potentials.[24] To stabilize PAHs, the CH atoms must be replaced by heteroatoms such as nitrogen (N)/sulfur/selenium, and two-dimensional (2D) acene analogues must be created by annealing the aromatic rings of PAHs onto adjacent rings.[25] This will effectively increase the intermolecular surface overlap.[26]

Among heteroatom-substituted PAHs, hexaazatriphenylene (HAT) is one of the smallest 2D N-containing polyheterocyclic aromatic systems and is an electron deficient, planar and rigid conjugated structure with superior pi–pi stacking ability.[24] HAT and its derivatives can be tuned by modifying the readily available six substituent groups resulting in different coordination structures.[27] This enables numerous applications for HAT and its derivatives in the development of n-type semiconductors, ligands for coordination chemistry, sensors, liquid crystals, magnetic materials and micro-porous for storing energy.[24,28–30] HAT based derivatives have also been used in optical applications due to their unique capability in recognizing metal ions and faster reaction toward heavy metals.[30,31] These derivatives synthesized with different coordination structures using phenyl or methyl groups have been investigated for selective detection of heavy metals such as Zinc (Zn) and Cd over other heavy metal ions.[32,33] However, there is no information available on the selective chemical detection capabilities of HAT derivatives towards Cu^{2+} ions with various modified structures such as quinone groups. Thus, an investigation to explore the capability of HAT derivatives to detect Cu^{2+} ions is highly desired.

In this work, a novel HAT derivative compound, naphtho[2,3-h]naphtho[2′,3':7,8]quinoxalino[2,3-*a*]naphtho[2′,3':7,8]quinoxalino[2,3-*c*]phenazine-5,10,15,20,25,30-hexaone (NQH) was synthesized for detecting Cu^{2+} ions using both optical and electrochemical detection techniques. NQH displays a high degree of metal–organic coordination interaction towards Cu^{2+} among many different ions in aqueous mixture. The optical detection capability of the NQH compound towards Cu^{2+} ions was investigated by using UV-Vis and fluorescence techniques. In addition, the electrochemical detection capability of the NQH compound towards Cu^{2+} ions was also investigated by using CV technique. For electrochemical measurements, a three-electrode electrochemical sensor fabricated using additive screen printing process was employed. Printed electronics (PE) enable the fabrication of sensing devices at relatively lower cost with attractive features such as flexibility and high throughput with minimal material wastage.[34–38] The optical and electrochemical measurements demonstrating the selectivity and sensitivity of NQH compound towards Cu^{2+} ions among various heavy metal ions is reported.

2. Experimental

2.1. Chemicals and materials

All chemicals were purchased from commercial sources and were used as received. Hexaketocyclohexane octahydrate, 1,2-phenylenediamine, glacial acetic acid, ethanol, and ethyl acetate, dichloro methane from Sigma Aldrich Chemical Company were used in the synthesis of NQH. All the metal salts including copper acetate ($Cu(CH_3COO)_2$), lithium chloride (LiCl), cobalt chloride ($CoCl_2$), ferrous chloride ($FeCl_2$), nickel chloride ($NiCl_2$), mercury chloride ($HgCl_2$), ferric chloride ($FeCl_3$) and lead acetate ($Pb(C_2H_3O_2)_2$) were obtained from Sigma Aldrich Chemical Company and dissolved in deionized (DI) water for preparing the stock solutions, for concentrations ranging from 100 μM to 1 μM. The stock solutions of metals prepared using DI water, with have pH 7, were used directly for experiments/measurements without adding any buffers (used to alter the pH) to avoid cross-contaminations. Dimethyl sulfoxide (DMSO) and dimethyl sulfoxide-d_6 (DMSO-d_6) from Sigma Aldrich Chemical Company were used in the preparation of NQH and ^{1}HNMR as well as ^{13}C NMR experiments, respectively. A 127 μm thick transparent polyethylene terephthalate (Melinex® ST 506) from DuPont™ Teijin Films was employed as the substrate, for fabricating a flexible three electrode configuration electrochemical sensor. A flexible conductive silver ink (Ag 800) from Applied Ink Solutions was used for metalizing the counter electrode. A carbon conductive ink (DuPont 7105) and an Ag/AgCl paste (DuPont 5874) from DuPont™ was used as the working and reference electrode, respectively. Isopropyl alcohol and ethylene glycol di-acetate from Sigma Aldrich Chemical Company was used for cleaning the substrate and screen-printing press, respectively.

2.2. Apparatus

A JEOL model JNMECP400 instrument was used to collect the ^{1}H NMR and ^{13}C NMR spectra of the NQH at 400 MHz in DMSO-d_6. The NQH samples were introduced in the JEOL instrument at 5–10 mL min^{-1} when the source temperature was maintained at 80 °C with nebulizing gas supply at 250 L h^{-1}. UV-Vis absorbance spectra of the chemical compounds were recorded using a Varian Cary 50 Bio Spectrophotometer. A Varian Cary Eclipse fluorescence spectrometer was used to collect the fluorescence spectra. Mass spectrometry was performed using a Waters SYNAPT G1 HDMS™ instrument with electrospray ionization (ESI). The electrospray capillary voltage was set to 2 kV with a desolvation temperature of 150 °C while the sampling and extraction cones were set at 40 V and 1 V, respectively. Interface 1010E from Gamry instruments was used as a potentiostat to measure and record CV as well as EIS responses of the NQH drop-casted electrochemical sensor. A spring-loaded small outline integrated circuit (SOIC) test clip from Pomona Electronics 6108 was used to connect the electrochemical sensor to the potentiostat. All the probes and wires were calibrated prior to obtaining the measurements.

2.3. Synthesis of NQH

Fig. 1 shows the synthesis of the NQH ($C_{48}H_{18}N_6O_6$) compound. To synthesize NQH, initially 1,2-phenylenediamine (10.4 g, 96.0 mmol) and hexaketocyclohexane octahydrate (10.0 g, 32.0 mmol) were refluxed particularly in 1 : 1 glacial acetic acid/ethanol (500 mL) solvents at 140 °C for 3 h to reduce the total

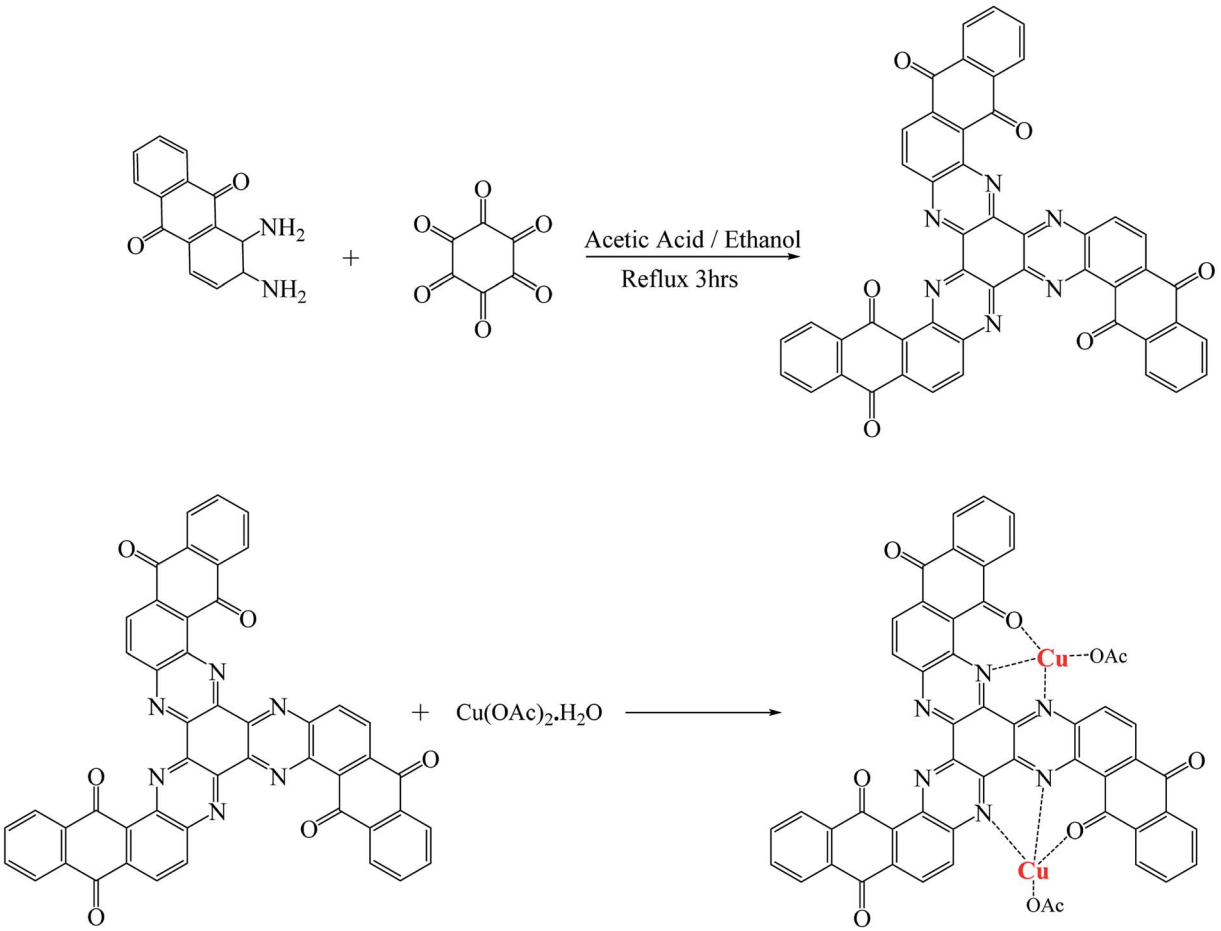

Fig. 1 Schematic representation of the synthesis of NQH.

reaction time as well as to make the reaction more shifted toward Schiff base formation. After refluxing, the mixture was filtered using a 25 μm pore size filter paper to remove the solvents and the remaining solid which is a HAT derivative. The mixture was washed with hot glacial acid (200 mL) to remove the impurities/residues and dried under vacuum for 1 h. The precipitated powder obtained after drying in vacuum was then purified by column chromatography filled with silica gel using ethyl acetate, dichloro methane of 1 : 1 (v/v) to produce a yellow colored liquid, NQH. Depending upon the requirement of the characterizations such as ^{1}NMR, mass spectroscopy or UV-Vis, the obtained NQH liquid was converted to powder by further vacuum drying and dissolved in solvents such as DMSO-d_6 or methanol or ethanol.

The prepared NQH was characterized by ^{1}H NMR as well as ^{13}C NMR spectroscopy to confirm its structure. The corresponding peaks for the NQH structure were identified at ^{1}H NMR (400 MHz, DMSO-d_6): δ 8.16–8.30 (2H, m, aromatic), 8.09–8.13 (1H, d, J 1/4 9.0 Hz, aromatic), 7.86–7.95 (4H, m, aromatic) ppm as shown in Fig. 2(a). The peaks observed for ^{13}C NMR (75 MHz, DMSO-d_6, d ppm): δ 126.8, 127.1, 132.1, 133.6, 135.5, 135.7, 137.1, 137.9 ppm corresponds to –C–N, –C═O, –C–C, –C–H groups as shown in Fig. 2(b).

2.4. Electrochemical sensor fabrication

A schematic of the three-electrode electrochemical sensor with a working electrode (1700 μm radius), a counter electrode (inner and outer radius of 2900 μm and 3900 μm) and a reference electrode (1000 μm width) is shown in Fig. 3(a). A screen-printing press (AMI MSP 485) from Affiliated Manufacturers Inc. was first calibrated and a stainless-steel screen frame fabricated at Microscreen®, with electrode designs was installed. The wire diameter, mesh count and deflection angle of screen frame were 28 μm, 325 and 22.5°, respectively. The three inks carbon, Ag 800 and Ag/AgCl were screen printed, as the working, counter and reference electrodes, directly onto PET due to their better adhesion properties. The samples were then cured in a VWR oven at 100 °C for 10 minutes. The photograph of the screen-printed electrochemical sensor is shown in Fig. 3(b). A 160 μL NQH in ethanol solution was drop-casted on the working electrode of the printed sensor at 80 °C. Later, 120 μL of DI water was initially drop casted on the sensor to obtain a reference/blank signal. Then, 120 μL of varying concentrations of Cu^{2+} and other heavy metals were drop casted on the NQH and their voltammetry responses were recorded at a scan rate of 50 mV s^{-1} and between potentials ranging from −0.3 V to 1 V.

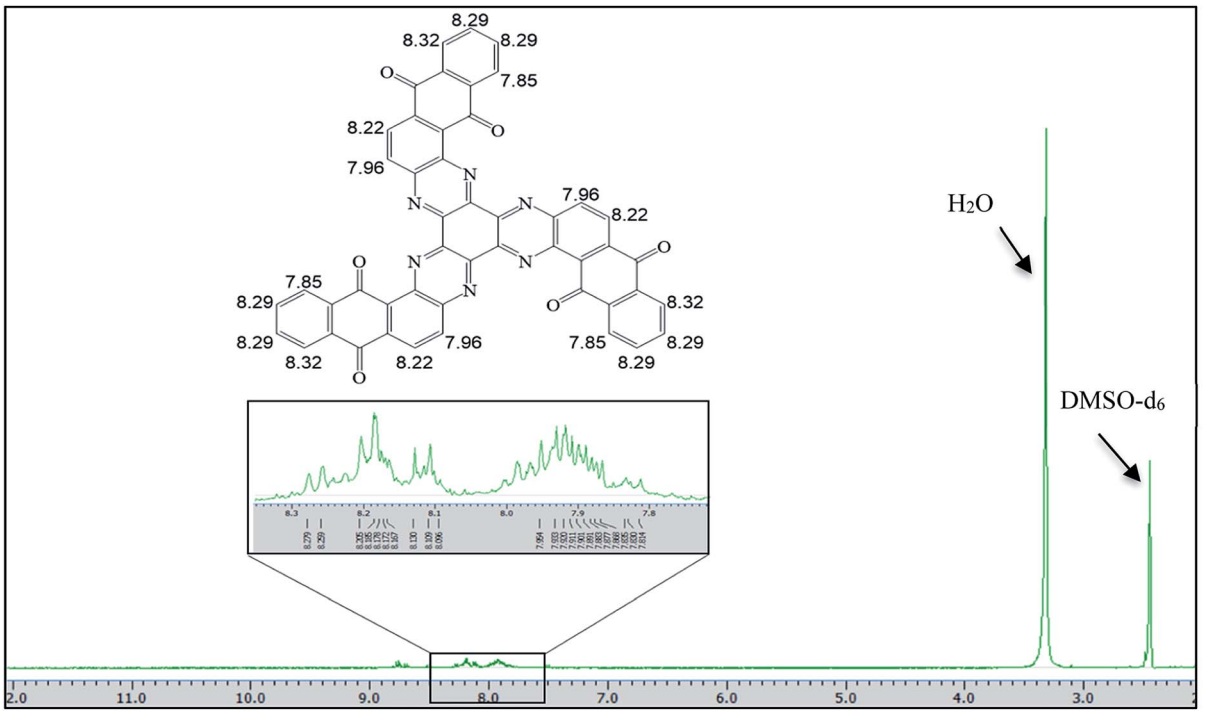

(a)

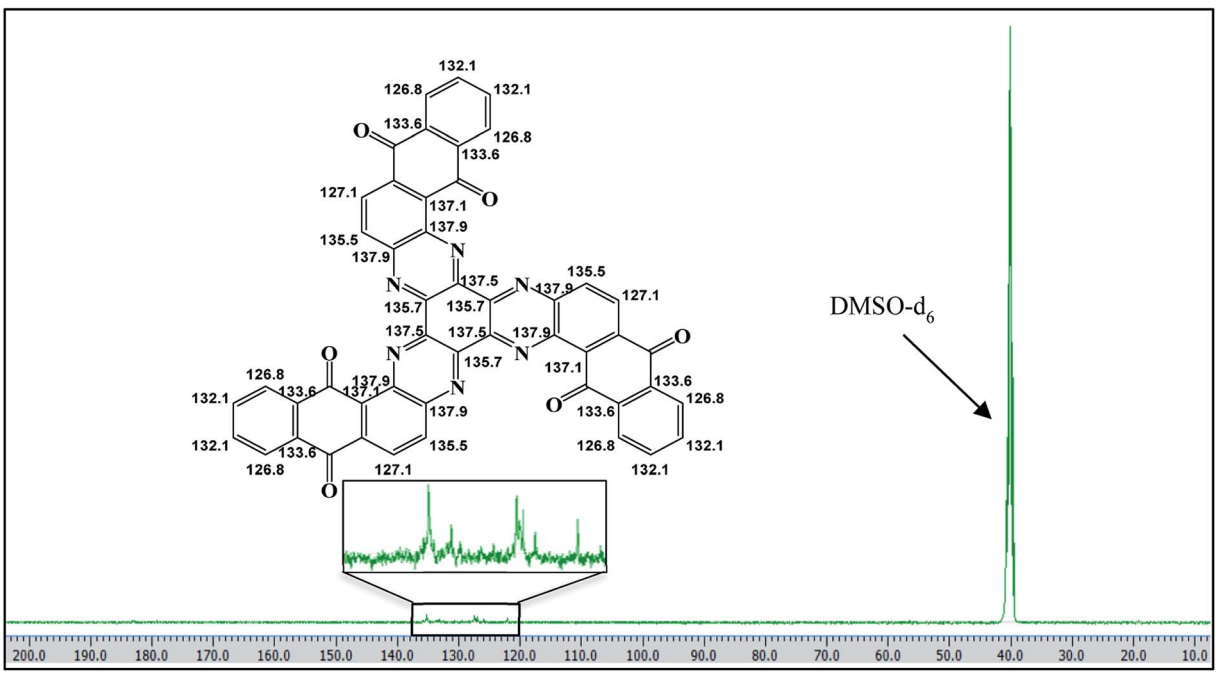

(b)

Fig. 2 (a) ^{1}H-NMR and (b) ^{13}C-NMR spectra of NQH.

3. Results and discussion

3.1. Monitoring changes in optical properties of NQH upon exposure to Cu^{2+}

The selectivity and the sensitivity of the NQH compound towards different heavy metals was investigated by using UV-Vis absorbance spectroscopy. Initially, UV-Vis absorption spectra of NQH was recorded in the presence of 100 μM concentration of metal ions including Cu^{2+}, Co^{2+}, Ni^{2+}, Fe^{2+}, Fe^{3+}, Li^{1+}, Pb^{2+}, and Hg^{2+} in aqueous media (Fig. 4(a)). An absorbance peak at ~435 nm was observed for the NQH compound. No color change as well as no shift in peak was observed in the presence

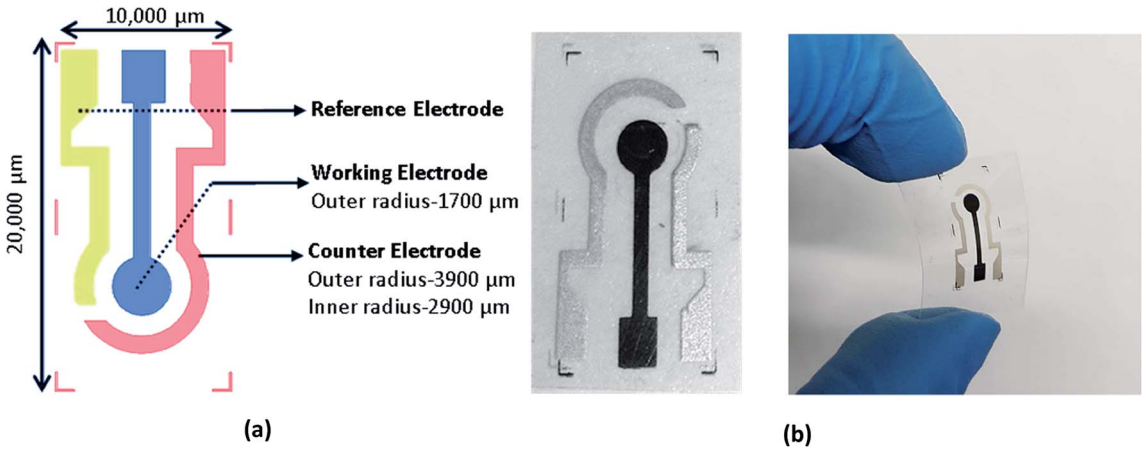

Fig. 3 (a) Schematic and (b) photograph of the screen printed electrochemical sensor.

of NQH with various metal ions except Cu^{2+}. However, when the Cu^{2+} metal ions were added to the NQH compound, a change in color from yellow to brown as well as a shift in the absorbance peak from ~435 nm to ~485 nm was induced, implying a high selectivity of NQH towards Cu^{2+}. This facilitates the synthesized NQH compound as a colorimetric sensor for the detection of Cu^{2+}. The color change arises from the d–d electron transitions that occurs due to the absorbance of the light.[39] Furthermore, the shift in the absorbance peak for NQH + Cu^{2+} is due to metal-to-ligand charge-transfer (MLCT) complexes arising from the transfer of electrons from molecular orbitals in metal to molecular orbitals in ligand.[40,41]

In order to determine the sensitivity of NQH toward Cu^{2+}, a metal titration experiment was conducted using various Cu^{2+} concentrations ranging from 0 µM to 100 µM. Fig. 4(b) shows that the absorbance peak at 485 nm increased linearly with the increase in the concentration of Cu^{2+}. An increase in the 485 nm absorbance peak from ~0.2 to ~0.3 was observed when the concentrations of Cu^{2+} were increased from 0 µM (blank) to 100 µM. This resulted in a sensitivity of 0.0007/µM and a correlation coefficient of 0.98 for the colorimetric sensor (Fig. 5). The limit of detection (LOD) and limit of quantification (LOQ) were mathematically calculated using eqn (1) and eqn (2), respectively.[42]

$$\mathrm{LOD} = 3.3 \times \frac{s}{m} \quad (1)$$

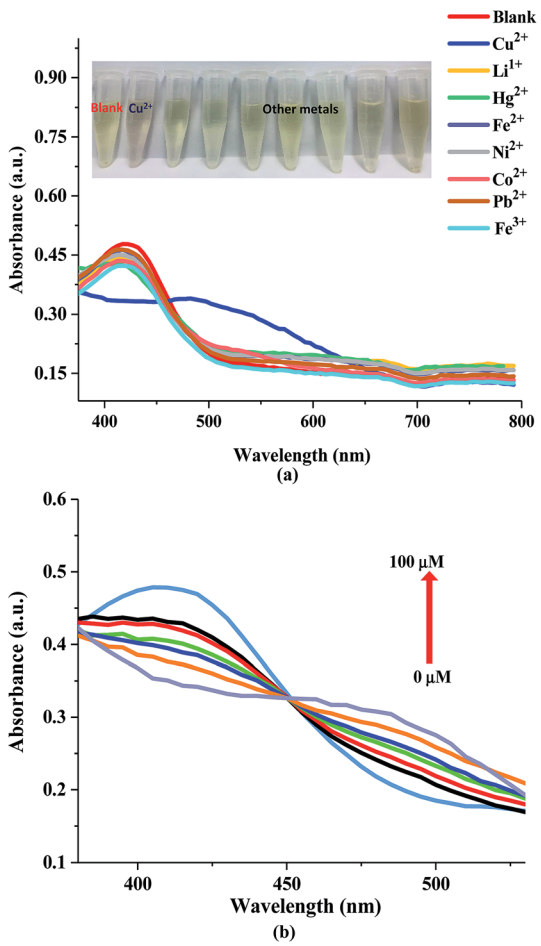

Fig. 4 (a) UV-Visible absorbance spectra of NQH in the presence of different metal ions and (b) UV-Visible absorbance spectra of NQH compound with varying Cu^{2+} concentrations.

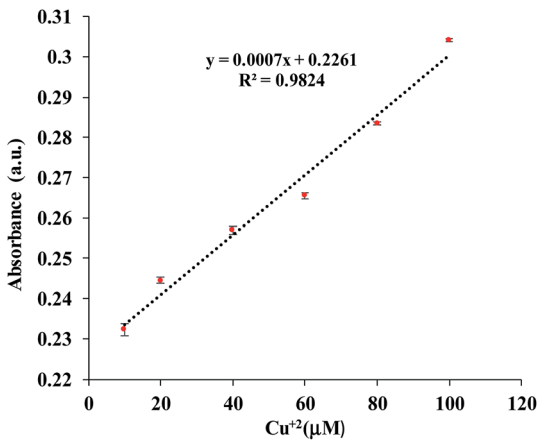

Fig. 5 Linear plot for determination of LOD and LOQ.

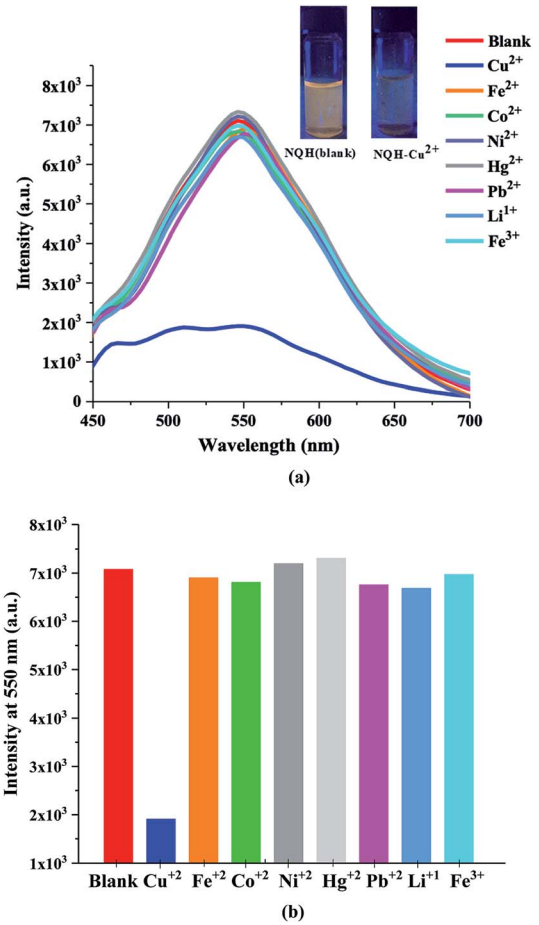

Fig. 6 (a) and (b) Fluorescence emission spectra of NQH in the presence of different metal ions.

$$\mathrm{LOQ} = 10 \times \frac{s}{m} \tag{2}$$

where s is the standard deviation (5 samples) of the blank, and m is the slope of the regression line y. The LOD and LOQ for Cu^{2+} were found to be 3.32 μM and 10.06 μM, respectively, which was lower than the toxicity levels of copper in drinking water (20–30 μM) according to the environmental protection agency (EPA) as well as World Health Organization (WHO).[43,44]

3.2. Fluorescence study of NQH compound

The fluorescence response of NQH compound towards various heavy metal ions was investigated at an excitation wavelength of 435 nm as shown in Fig. 6(a) and (b). The NQH compound exhibited a strong emission peak with maximum intensity of ~7 × 10^3 (a.u.) at 550 nm. The similar strong emission peaks at ~550 nm were observed for NQH mixed with other heavy metals such as Co^{2+}, Ni^{2+}, Fe^{2+}, Fe^{3+}, Li^{1+}, Pb^{2+}, and Hg^{2+}. However, upon adding NQH compound with Cu^{2+}, the emission peak was significantly quenched by ~74.5% when compared to the emission peak intensity of NQH compound, thus showing very high selectivity towards Cu^{2+} ions over other metals (Fig. 6(a) and (b)).

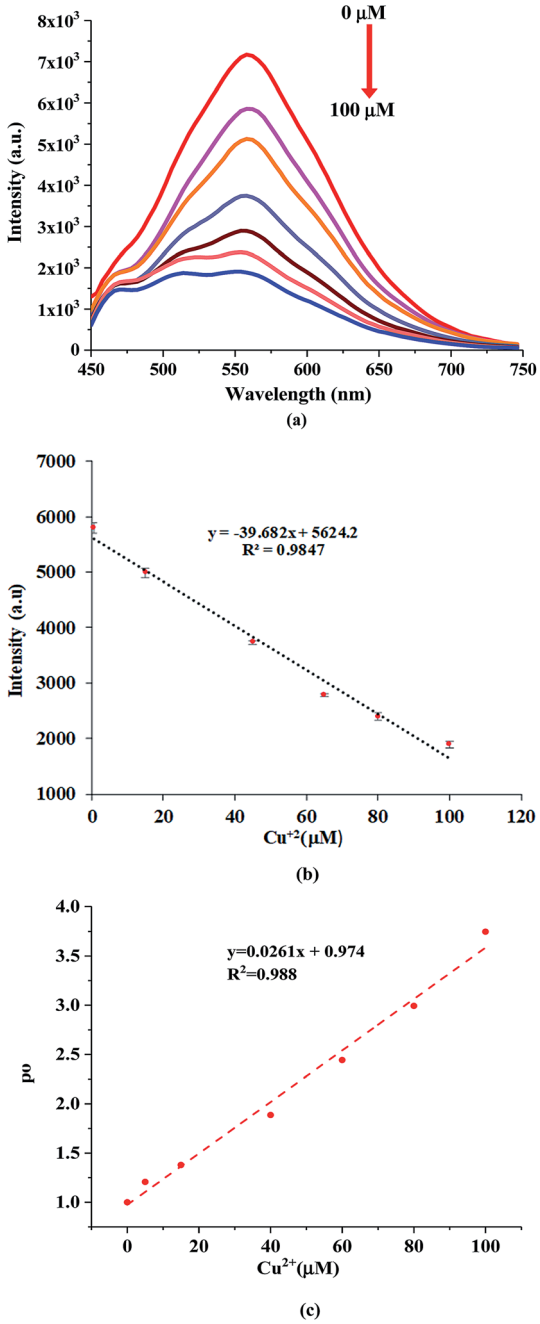

Fig. 7 (a) Fluorescence emission spectra of NQH compound towards varying Cu^{2+} ionic concentrations and (b) the linear plot for calculating LOD and LOQ and (c) relative quantum yield.

The fluorescence quenching arises from the addition of a quenching agent Cu^{2+} to the fluorophore NQH, which can be interpreted in terms of chelation-induced fluorescence quenching. The fluorophore NQH itself is fluorescent when its receptor sites (nitrogen groups) are free. In the presence of Cu^{2+} metal ions, the fluorescence intensity of the NQH is lowered due to chelation of the Cu^{2+} ions to the receptor unit of the sensor. NQH compound with Cu^{2+} forms a ground-state complex, which can reduce the electron density of the complex causing the intramolecular charge-transfer effect which in turn

quenches the fluorescence intensity.[31,45–47] In addition, Cu^{2+} is a paramagnetic cation consisting of an unfilled d shell (d^9) and has the ability to quench the emission of nearby or surrounding fluorophores strongly through electron transfer processes.[48] When Cu^{2+} binds to NQH, the paramagnetic nature of Cu^{2+} with the unfilled d^9 shell could facilitate the energy or electron transfer through a non-radiative deactivation channel, thereby quenching the fluorescence of NQH.[49]

The sensitivity of the NQH towards the increasing concentrations of Cu^{2+} from 0 μM to 100 μM was shown in Fig. 7(a). A decrease in the fluorescence intensity from 7.07×10^3 to 1.8×10^3 was observed as the concentration of the Cu^{2+} ions were increased from 0 μM to 100 μM at ~550 nm. This resulted in a sensitivity of 39.7/μM and a correlation coefficient of 0.98 for the fluorescence chemo sensor (Fig. 7(b)). A LOD and LOQ of 2.2 μM and 6.9 μM was mathematically calculated using eqn (1) and eqn (2), respectively. In addition, the dynamic quenching process (Fig. 7(c)) was described using the Stern–Volmer relationship in which the quantum yield and the fluorescence intensity are related by eqn (3).[50–52]

$$\frac{\Phi_0}{\Phi} = \frac{I_0}{I} = 1 + K_{sv}[Q] \quad (3)$$

where ϕ_0 and ϕ are the fluorescence quantum yields in the absence and presence of quencher (Cu^{2+} ions), respectively; I_0 and I are the fluorescence intensities of NQH in the absence and presence of quencher, respectively; Q is the concentration of the Cu^{2+} and K_{SV} is the quenching rate constant. It was observed from Fig. 7(c) that the relative quantum yield $\left(\frac{\Phi_0}{\Phi}\right)$ or relative fluorescence intensity $\left(\frac{I_0}{I}\right)$ increased as the concentration of the Cu^{2+} ions were increased resulting in a quenching rate constant of 0.026 and a correlation coefficient of 0.988. From eqn (3), it can be concluded that the quantum yield (ϕ) is inversely proportional to the concentration of Cu^{2+} ions.

3.3. Binding stoichiometry

In order to determine the coordination ratio or binding stoichiometry between the NQH compound and Cu^{2+}, Job's plot experiment was performed (Fig. 8).[53,54] In the Job's plot experiment, the prepared stock solution of NQH was 1 M which was then diluted to different concentrations from 0.1 mM to 0 mM by adding ethanol. Then Cu^{2+} ions from 0 μM to 100 μM were added to the diluted solutions of NQH in such a way that the total molarity of [NQH] + [Cu^{2+}] was fixed at 0.1 mM resulting in mole fractions of [Cu^{2+}]/([Cu^{2+}] + [NQH]) between 0.1–1.0. The absorbance of the [NQH] + [Cu^{2+}] complex with different mole fractions was recorded at 485 nm. A maximum absorbance was observed at a mole fraction of 0.75 indicating the 1 : 2 stoichiometry for NQH and Cu^{2+} complexation. The 1 : 2 stoichiometry complexation between NQH and Cu^{2+} was further confirmed by

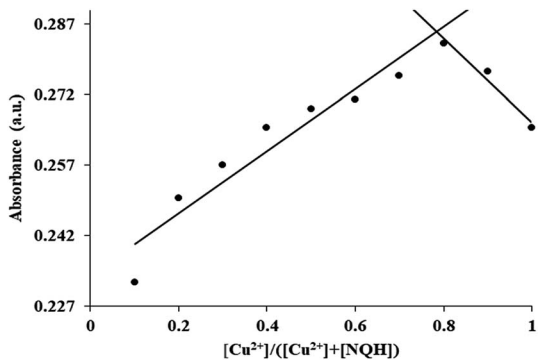

Fig. 8 Job's plot for determining the stoichiometry of NQH and Cu^{2+}.

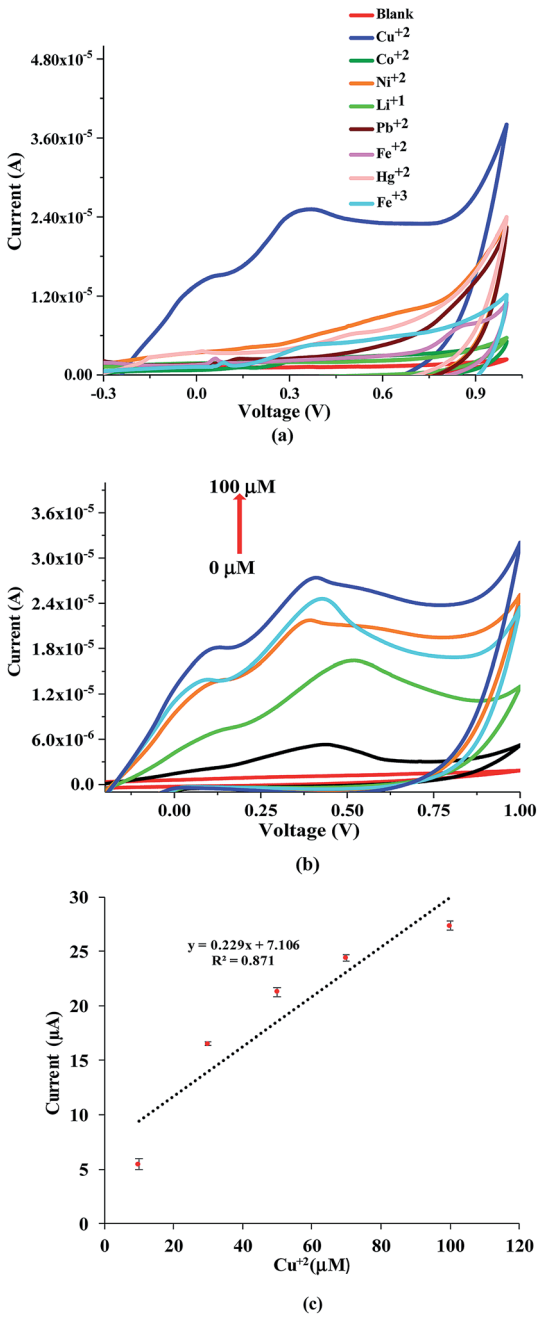

Fig. 9 (a) Cyclic voltammogram of NQH in presence of different metal ions, (b) cyclic voltammetry response of NQH towards varying Cu^{2+} concentrations and (c) linear plot for determination of LOD and LOQ.

Table 1 Comparison summary of the performances of some reported Cu^{2+} sensors

Cu^{2+} Sensitive Material	Response	Stoichiometry binding	LOD (μM)	Sensitivity	Cu Concentration Range (μM)	References
Pyridoxal derived	Fluorescence intensity	1 : 1	1.89	0.0044	0–30	56
Julodine Schiff base	Colorimetric	1 : 1	23.5	0.0007	20–200	57
Vitamin B6 cofactor	Colorimetric	1 : 1	1.01	0.0002	5–55	58
Dansyl derivative	Fluorescence	—	0.979	∼7.8	∼5–16	59
Pyrazole system	Fluorescence	1 : 1	24	—	0–60	60
Uracil nitroso amine	Colorimetric	1 : 1	10	0.000471	—	61
Salicylaldehyde Schiff base	Colorimetric	1 : 1	8.77	0.0023	0–80	62
NQH	Colorimetric/ fluorescence intensity/ electrochemical	2 : 1	3.32 2.2 0.78	0.0007 39.7 0.23	0–100	(Present work)

performing MALDI-TOF mass spectroscopy. The mass spectroscopy was conducted for NQH ($C_{48}H_{18}N_6O_6$) and Cu^{2+} mixture with a binding ratio of 1 : 2 moles. As shown in Fig. S1(a),† a characteristic peak was observed at 775.0594 *m*/*z* which corresponds to the free $[NQH + H]^+$. When Cu^{2+} was added to the NQH solution, a new characteristic peak was obtained at 1251.7280 *m*/*z* corresponding to $[NQH–Cu_2(CH_3COO)_5\ 3H_2O + H]^+$ as shown in Fig. S2(b).† This result confirms the existence of one molecule NQH binding with two Cu^{2+} ions.

3.4. Electrochemical study

The CV measurements were recorded for the printed sensor towards different heavy metals including Cu^{2+}, Ni^{2+}, Co^{2+}, Fe^{2+}, Fe^{3+}, Li^{1+}, Ni^{2+}, Hg^{2+} and Pb^{2+}, to test the selectivity of NQH compound towards Cu^{2+} ions. The CV responses towards various heavy metals of 100 μM were recorded from −0.3 V to 1 V at a scan rate of 50 mV s^{-1}. A peak at ∼0.4 V was obtained for the Cu ions and no affinity/response towards other metals were detected as shown in Fig. 9(a). Also, the anodic zone showed a clear oxidation peak at 0.4 V corresponding to Cu(I)/Cu(II). This behavior clearly demonstrated that Cu is present in the complex as Cu^{2+} ion which is comparable with previous literature.[55] These results clearly indicate that the NQH drop casted sensor possess excellent selectivity towards Cu^{2+}. The selectivity of NQH compound towards only Cu^{2+} ions is due to the chelation of the Cu^{2+} ions by the free nitrogen groups resulting in a complex formation between nitrogen and Cu^{2+} ions.

Fig. 9(b) shows the CV response of the NQH drop-casted electrochemical sensor towards various ionic concentrations of Cu^{2+} ion solutions. An increase in the prominent peak current from 1.1 μA to 27.4 μA was observed at ∼0.4 V when the Cu^{2+} ion concentrations were increased from blank (DI water) to 100 μM, respectively. A sensitivity of 0.23 μA μM^{-1} and a correlation coefficient of 0.87 was obtained for the electrochemical sensor (Fig. 9(c).) In addition, a LOD of 0.78 μM and LOQ of 2.37 μM was calculated which is below the Cu^{2+} toxicity levels set by EPA and WHO.

In addition, the EIS response were recorded at 1 V and operating frequency ranging from 20 Hz to 20 kHz to verify the selectivity of the NQH drop-casted sensor (Fig. S2†). A reference impedance signal of 713 kΩ was measured initially at 20 Hz by drop casting DI water on the sensor. Then, a very high impedance of 171 kΩ was observed at 20 Hz for Cu^{2+} when compared to impedance of 31 kΩ, 57 kΩ, 39 kΩ, 53 kΩ, 16 kΩ and 66 kΩ for various metal ions Ni^{2+}, Co^{2+}, Li^{1+}, Fe^{3+}, Hg^{2+} and Pb^{2+}, respectively. This results clearly indicate that the sensor was able to distinguish Cu^{2+} among various other metal ions. A comparison summary of the current work with some reported Cu^{2+} sensors is shown in Table 1. It can be noticed that the developed Cu^{2+} sensor of this work has an appreciable LOD and sensitivity when compared to some of the reported Cu^{2+} sensors.

4. Conclusion

A novel HAT derivative based NQH compound was synthesized for selective detection of Cu^{2+} ions in water. The capability of the NQH compound to be employed as a colorimetry, chemofluorescence and electrochemical sensor for the detection of Cu^{2+} was demonstrated by performing UV-Vis absorbance, fluorescence intensity, and cyclic voltammetry measurements. UV-Vis absorbance and fluorescence of NQH toward Cu^{2+} showed a good linearity with a detection limit of 3.32 μM and 2.20 μM, respectively. Job's plot and mass spectroscopy results revealed a 1 : 2 stoichiometry complexation between NQH and Cu^{2+}. In addition, the selectivity and sensitivity of NQH compound towards Cu^{2+} ions was further confirmed by performing cyclic voltammetry on a screen printed flexible and planar electrochemical sensor. Future work includes optimization of the performance of the sensors in terms of sensitivity and LOD as well as LOQ by varying the quantity of NQH compound specifically for UV-Vis absorbance as well as fluorescence measurements and by adding the salts to increase the electrolytic activity for electrochemical measurements.

Conflicts of interest

There are no conflicts to declare.

References

1 Y. Shan, M. Tysklind, F. Hao, W. Ouyang, S. Chen and C. Lin, *J. Soils Sediments*, 2013, **13**(4), 720–729.

2 P. B. Tchounwou, C. G. Yedjou, A. K. Patlolla and D. J. Sutton, *Molecular, clinical and environmental toxicicology*, Springer, 2012, pp. 133–164.
3 P. C. Nagajyoti, K. D. Lee and T. V. M. Sreekanth, *Environ. Chem. Lett.*, 2010, **8**(3), 199–216.
4 Z. Rahman and V. P. Singh, *Environ. Monit. Assess.*, 2019, **191**(7), 419.
5 R. Chander, S. Naveen, K. Arora and R. Kothari, *Environmental Biotechnology: For Sustainable Future*, 2018.
6 R. A. Festa and D. J. Thiele, *Curr. Biol.*, 2011, **21**(21), R877–R883.
7 B. R. Stern, *J. Toxicol. Environ. Health, Part A*, 2010, **73**(2–3), 114–127.
8 N. Barnes, R. Tsivkovskii, N. Tsivkovskaia and S. Lutsenko, *J. Biol. Chem.*, 2005, **280**(10), 9640–9645.
9 I. F. Scheiber, J. F. B. Mercer and R. Dringen, *Prog. Neurobiol.*, 2014, **116**, 33–57.
10 D. J. Waggoner, T. B. Bartnikas and J. D. Gitlin, *Neurobiol. Dis.*, 1999, **6**(4), 221–230.
11 J. Emerit, M. Edeas and F. Bricaire, *Biomed. Pharmacother.*, 2004, **58**(1), 39–46.
12 H. Zischka and C. Einer, *Int. J. Biochem. Cell Biol.*, 2018, **102**, 71–75.
13 V. Chrastny and M. Komarek, *Chem. Pap.*, 2009, **63**(5), 512–519.
14 C. Karadas, O. Turhan and D. Kara, *Food Chem.*, 2013, **141**(2), 655–661.
15 L. Zhao, S. Zhong, K. Fang, Z. Qian and J. Chen, *J. Hazard. Mater.*, 2012, **239**, 206–212.
16 R. L. Nixon, S. L. Jackson, J. T. Cullen and A. R. S. Ross, *Mar. Chem.*, 2019, 103673.
17 K. T. Makhmudov, R. A. Alieva, S. R. Gadzhieva and F. M. Chyragov, *J. Anal. Chem.*, 2008, **63**(5), 435–438.
18 M. Z. Atashbar, B. E. Bejcek and S. Singamaneni, *IEEE Sens. J.*, 2006, **6**(3), 524–528.
19 B. Ziaie, A. Baldi and M. Z. Atashbar, *Springer handbook of nanotechnology*, 2004, pp. 147–184.
20 Y. Fu, C. Fan, G. Liu and S. Pu, *Sens. Actuators, B*, 2017, **239**, 295–303.
21 S. Chaiyo, W. Siangproh, A. Apilux and O. Chailapakul, *Anal. Chim. Acta*, 2015, **866**, 75–83.
22 J. Wu, W. Pisula and K. Mullen, *Chem. Rev.*, 2007, **107**(3), 718–747.
23 J. E. Anthony, *Chem. Rev.*, 2006, **106**(12), 5028–5048.
24 J. L. Segura, R. Juarez, M. Ramos and C. Seoane, *Chem. Soc. Rev.*, 2015, **44**(19), 6850–6885.
25 L. Zhang, Y. Cao, N. S. Colella, Y. Liang, J. L. Bredas, K. N. Houk and A. L. Briseno, *Acc. Chem. Res.*, 2015, **48**(3), 500–509.
26 L. Chen, Y. Hernandez, X. Feng and K. Mullen, *Angew. Chem., Int. Ed.*, 2012, **51**(31), 7640–7654.
27 S. Kitagawa and S. Masaoka, *Coord. Chem. Rev.*, 2003, **246**(1–2), 73–88.
28 B. R. Kaafarani, *Chem. Mater.*, 2010, **23**(3), 378–396.
29 T. Ishi-i, K. Yaguma, R. Kuwahara, Y. Taguri and S. Mataka, *Org. Lett.*, 2006, **8**(4), 585–588.
30 X. Y. Yan, M. Di Lin, S. T. Zheng, T. G. Zhan, X. Zhang, K. Da Zhang and X. Zhao, *Tetrahedron Lett.*, 2018, **59**(7), 592–604.
31 Y. Li, L. Le Yang, K. Liu, F. Y. Zhao, H. Liu and W. J. Ruan, *New J. Chem.*, 2015, **39**(4), 2429–2432.
32 X. H. Zhang, Q. Zhao, X. M. Liu, T. L. Hu, J. Han, W. J. Ruan and X. H. Bu, *Talanta*, 2013, **108**, 150–156.
33 X. H. Zhang, C. F. Zhao, Y. Li, X. M. Liu, A. Yu, W. J. Ruan and X. H. Bu, *Talanta*, 2014, **119**, 632–638.
34 Y. Meng, Z. B. Li, X. Chen and J. P. Chen, *Microsyst. Technol.*, 2015, **21**(6), 1241–1248.
35 V. S. Turkani, D. Maddipatla, B. B. Narakathu, T. S. Saeed, S. O. Obare, B. Bazuin and M. Z. Atashbar, *Nanoscale Adv.*, 2019, **1**, 2311–2322.
36 A. A. Chlaihawi, B. B. Narakathu, S. Emamian, B. J. Bazuin and M. Z. Atashbar, *Sens. Bio-Sens. Res.*, 2018, **20**, 9–15.
37 B. Narakathu, M. Sajini, A. Reddy, A. Eshkeiti, A. Moorthi, I. R. Fernando, B. P. Miller, G. Ramakrishna, E. Sinn, M. Joyce, M. Rebros, E. Rebrosova, G. Mezei and M. Atashbar, *Sens. Actuators, B*, 2013, **176**, 768–774.
38 M. M. Ali, D. Maddipatla, B. B. Narakathu, A. A. Chlaihawi, S. Emamian, F. Janabi, B. J. Bazuin and M. Z. Atashbar, *Sens. Actuators, A*, 2018, **274**, 109–115.
39 L. Fabbrizzi, M. Licchelli and P. Pallavicini, *Acc. Chem. Res.*, 1999, **32**(10), 846–853.
40 Q. Hu, K. Ma, Y. Mei, M. He, J. Kong and X. Zhang, *Talanta*, 2017, **167**, 253–259.
41 S. S. M. Rodrigues, D. R. Prieto, D. S. M. Ribeiro, E. Barrado, J. A. V. Prior and J. L. M. Santos, *Talanta*, 2015, **134**, 173–182.
42 L. H. Jin and C. S. Han, *Anal. Chem.*, 2014, **86**(15), 7209–7213.
43 https://archive.epa.gov/, (n.d.).
44 https://www.fda.gov/, (n.d.).
45 L. J. Fan, J. J. Martin and W. E. Jones, *J. Fluoresc.*, 2009, **19**(3), 555–559.
46 Y. Du, M. Chen, Y. Zhang, F. Luo, C. He, M. Li and X. Chen, *Talanta*, 2013, **106**, 261–265.
47 S. S. Tan, S. J. Kim and E. T. Kool, *J. Am. Chem. Soc.*, 2011, **133**(8), 2664–2671.
48 H. S. Jung, P. S. Kwon, J. W. Lee, J. I. I. Kim, C. S. Hong, J. W. Kim, S. Yan, J. Y. Lee, J. H. Lee, T. Joo and J. S. Kim, *J. Am. Chem. Soc.*, 2009, **131**, 2008–2012.
49 R. Kramer, *Angew. Chem., Int. Ed.*, 1998, **37**, 772–773.
50 W. S. Jeon, T. J. Park, K. H. Kim, R. Pode, J. Jang and J. H. Kwon, *Org. Electron.*, 2010, **11**, 179–183.
51 M. K. Seery, N. Fay, T. McCormac, E. Dempsey, R. J. Forster and T. E. Keyes, *Phys. Chem. Chem. Phys.*, 2005, **7**, 3426–3433.
52 E. J. Bowen, *Q. Rev., Chem. Soc.*, 1947, **1**, 1–15.
53 P. Job, *Ann. Chim. Phys.*, 1928, **9**, 113–203.
54 J. Plots, J. S. Renny, L. L. Tomasevich, E. H. Tallmadge and D. B. Collum, *Angew. Chem., Int. Ed.*, 2013, **52**(46), 11998–12013.
55 R. Fekri, M. Salehi, A. Asadi and M. Kubicki, *Polyhedron*, 2017, **128**, 175–187.
56 S. K. Sahoo, D. Sharma, A. Moirangthem, A. Kuba, R. Thomas, R. Kumar, A. Kuwar, H. J. Choi and A. Basu, *J. Lumin.*, 2016, **172**, 297–303.
57 Y. W. Choi, J. J. Lee, G. R. You, S. Y. Lee and C. Kim, *RSC Adv.*, 2015, **5**, 86463–86472.

58 D. Sharma, A. Kuba, R. Thomas, R. Kumar, H. J. Choi and S. K. Sahoo, *Spectrochim. Acta, Part A*, 2016, **153**, 393–396.
59 A. Thangaraj, V. Bhardwaj and S. K. Sahoo, *Photochem. Photobiol. Sci.*, 2019, **18**, 1533–1539.
60 T. Mistri, R. Alam, M. Dolai, S. K. Mandal, A. R. Khuda-Bukhsh and M. Ali, *Org. Biomol. Chem.*, 2013, **11**, 1563–1569.
61 S. R. Patil, J. P. Nandre, P. A. Patil, S. K. Sahoo, M. Devi, C. P. Pradeep, Y. Fabiao, L. Chen, C. Redshaw and U. D. Patil, *RSC Adv.*, 2015, **5**, 21464–21470.
62 K. Y. Ryu, J. J. Lee, J. A. Kim, D. Y. Park and C. Kim, *RSC Adv.*, 2016, **6**, 16586–16597.